Water Vapor Layers in STORM-FEST Rawinsonde Observations*

JOHN P. ISELIN

Department of Geological and Atmospheric Sciences, Iowa State University, Ames, Iowa

WILLIAM J. GUTOWSKI JR.

Department of Geological and Atmospheric Sciences, and Department of Agronomy, Iowa State University, Ames, Iowa

(Manuscript received 3 September 1996, in final form 28 December 1996)

ABSTRACT

The STORM-FEST (Fronts Experiment Systems Test) rawinsonde data were analyzed to determine the abundance and characteristics of moist layers within the troposphere. A moist layer was defined as a local maximum in relative humidity with lower relative humidity air above and below. Moist layers under the criteria occur in over half the soundings with an average location between 600 and 500 mb and an average thickness of approximately 120 mb. The layers also appeared to be more nearly aligned with isentropic, rather than isobaric, surfaces. Compositing of relative humidity profiles with a layer at approximately the same level showed an increase in lapse rate at the top of moist layers indicating that the layers are contained by dynamic mechanisms. In addition, there was no diurnal cycle to the characteristics of the layers. These factors suggest a close relationship between the layers and large-scale dynamics. An examination of spatial continuity suggests a horizontal scale of a few hundred kilometers. Their appearance poses a challenge for numerical modeling of atmospheric water vapor. Furthermore, limitations of the two types of rawinsonde instruments used in STORM-FEST are apparent in some characteristics of the layers, thus indicating instrumentation challenges posed by these structures for observing the atmospheric branch of the hydrological cycle.

1. Introduction

It is apparent on a partly cloudy day that the clouds appear at certain levels in the troposphere and not at other levels. This feature was used by Coakley and collaborators (Coakley and Bretherton 1982; Coakley and Baldwin 1983; Molnar and Coakley 1985) to retrieve cloud cover from satellite radiances. This characteristic of clouds (i.e. condensed water) to form into vertically stratified layers suggests that the water vapor field in which clouds are embedded may also form layers in the vertical. Such a characteristic, if prevalent, could pose a challenge for accurate modeling of the global water cycle. Gyakum (1987), for example, has shown how a layer of water vapor 20–150 mb thick produced an unforcasted snowstorm because the forecast model could not resolve the detailed vertical structure of the water vapor.

Layers might appear as part of a tendency, at times, for atmospheric large-scale dynamics to draw fields into narrow structures. As early as the mid-1950s, Welander (1955) used a two-dimensional model of an idealized fluid to show that a tracer is drawn into long narrow patterns. Kuettner (1959) speaks of a general characteristic of the atmosphere as being streaky, and Danielsen (1968) observed dry layers in the atmosphere due to tropopause folding, or the entrainment of dry stratospheric air into the troposphere. More recently, Newell et al. (1992) have diagnosed elongated, horizontal structures of water vapor transport, which they refer to as ''tropospheric rivers.'' Waugh and Plumb (1994) have shown that wind shear in the general circulation of the atmosphere can draw initially smooth fields of tracers into highly filamentary structures within 8–12 days. Finally, Newell et al. (1996) diagnosed over 500 layers of water vapor and other trace atmospheric components from 105 vertical profiles collected during aircraft flights for the Pacific Exploratory Mission A in the fall of 1991. These layers had an average thickness of about 400 m.

Project STORM-FEST (Project STORM-Fronts Experiment Systems Test) has produced an archive of atmospheric rawinsonde soundings that contains water vapor observations at relatively fine 10-mb vertical intervals. We have used this data to examine the characteristics of moist (high humidity) layers that occurred

* Journal paper No. J-17019 of the Iowa Agriculture and Home Economics Experiment Station, Ames, Iowa.

Corresponding author address: Dr. William J. Gutowski, Department of Geological and Atmospheric Sciences, Iowa State University, 3010 Agronomy Hall, Ames, IA 50011-1010.

during the STORM-FEST project period, 1 February–15 March 1992. Although the STORM-FEST data archive covers only a 6-week period, its weather was fairly typical for the central United States, so the results found here may be representative of water vapor behavior over a broader span of space and time. In the next section, we describe relevant characteristics of STORM-FEST and its data archive. In that section, we also review accuracy assessments of rawinsonde humidity measurements, because difficulties in observing atmospheric water vapor appear to affect the results reported here. We give our definition of a moist layer in section 3 and the results of our analysis in section 4. In the final section, we offer some implications of the results of our analysis.

2. Data

a. STORM-FEST dataset

The STORM-FEST experiment was conducted by the U.S. Weather Research Program (USWRP) to study winter storms in the middle of the United States. The purpose of the study was to ''investigate the structure and evolution of fronts, embedded precipitation and associated mesoscale phenomena in winter storms over the central United States'' (Cunning et al. 1993). As part of the STORM-FEST data collection phase, fixed-station rawinsonde soundings were used. The STORM-FEST rawinsonde network included operational National Weather Service (NWS) stations distributed across the Midwest and High Plains of the central United States. The network's horizontal resolution was enhanced by the addition of 12 Cross-chain Loran Atmospheric Sounding Stations (CLASS; Fig. 1) established for the duration of STORM-FEST. A 1000 km (zonal) $\times$ 800 km (meridional) subsection of the region, including 11 NWS stations and all of the CLASS stations, was used for the present study (Fig. 1).

Standard STORM-FEST soundings occurred every day at 0000 UTC and 1200 UTC during the period 1 February–15 March 1992. Additional soundings were launched during intensive observation periods (IOP), which were established to study the characteristics of the planetary boundary layer, fronts, and major wintertime storms. The IOPs were also used to calibrate and compare instruments. IOPs included soundings as often as every 3 h and contained 31% of the total soundings available. The USWRP compiled all of the upper-air data into a composite dataset using the National Center for Atmospheric Research (NCAR) CLASS format. Reported values were interpolated to 10-mb levels. Thus, the STORM-FEST composite data contained potentially high resolution on a regular vertical grid, both features making it amenable to our analysis. USWRP performed manual checks on all soundings and flagged each one according to its physical reasonableness. Data were marked as 1) physically reasonable, 2) questionable, 3) in error, 4) missing, or 5) unchecked (STORM 1996). We used only data that was indicated as physically reasonable in our analysis.

FIG. 1. Domain used for analysis outlined by the box. Stations marked N are NWS stations, and stations marked C are CLASS stations.

b. Reliability of rawinsonde measurements

Because our analysis focuses on fluctuations of water vapor fields with height, it is important to understand the accuracy and limitations of rawinsonde measurements. Of the quantities given in the STORM-FEST dataset, the three that are of interest in this study are pressure, temperature, and relative humidity. Relative humidity (RH) is of course the most difficult to measure (e.g., Pratt 1985). Nearly all STORM-FEST stations used one of two RH instruments: the VIZ carbon hygristor (NWS sondes) or the Vaisala humicap (CLASS sondes). The exception was the NWS station at Amarillo, Texas, which used rawinsondes made by the Space Data Division (SDD) of the Orbital Sciences Corporation. Differences in measurement characteristics among the instruments are relevant to the results.

Elliot and Gaffen (1991) report that, as a whole, humidity sensors are accurate to within 2%. However, Wade (1995) shows that, under certain conditions, the VIZ carbon hygristor used in the NWS soundings contains significant errors. In the VIZ carbon hygristor, one source of error comes from the use of electrical resistance to infer atmospheric relative humidity. The carbon hygristor changes its resistance as a function of both RH and temperature, so an algorithm is used to convert the recorded electrical resistance and temperature into RH. The algorithm uses a ratio of the reported resistance

to a reference resistance (referred to as the ''lock-in resistance''). Because the resistance's dependence on RH and temperature is not a readily defined analytical function, polynomial expansions are used to approximate the functional relationship. Thus, errors in the resistance and temperature measurements, the reduction algorithm, and the lock-in resistance all can lead to errors in the recorded RH. The largest error is a high bias at humidities below 20% due to an error in the algorithm to convert resistance and temperature into relative humidity. The error also causes the VIZ instrument to appear insensitive to RH fluctuations when RH is below 20% (Wade 1994). In addition, Marchgraber and Grote (1965) showed that 90% of the response of the carbon hygristor element to step changes in RH took approximately 2.8 s at 25°C, whereas the same response took 114 s at −20°C. Thus, the response of the carbon hygristor is much slower at lower temperatures, which are typically at higher altitudes. Using the average NWS balloon ascent rate from the STORM-FEST dataset of 4.5 m s^{-1}, this corresponds to a balloon rise of 12.6 m at 25°C and 513 m at −20°C. These biases will be evident in some of the results of this study.

Wade and Schwartz (1993) have also found that the VIZ instrument has a low bias near saturation. This was caused when the VIZ 1492 model replaced the older VIZ 1392 in 1988–89. The error arises from a change in the frequency control circuitry of the two instruments, coupled with the continued use of the model 1392 reduction algorithm to convert resistance into RH. One consequence of these operational procedures is that the VIZ instrument rarely reports RH above 95%. In addition, Wade (1995) shows that an error can occur in the soundings if the actual lock-in resistance differs from that used in the reduction algorithm. The lock-in resistance of every instrument is not measured. Instead, the average lock-in resistance of 1% of a production lot is used as the lock-in resistance for all instruments in the lot. This error is most significant at lower RH (potentially in excess of 12%) and exceeds the NWS error standard of 3% at 33% RH if the lock-in resistance is in error of ±600 ohm. It is not known how much variability there is in lock-in resistance within a production lot. However, Wade (1995) showed that the lock-in resistance may vary as much as 100% (10 000 ohm).

SDD sondes flown at Amarillo, Texas, also used the VIZ carbon hygristor. Wade (1995) has shown that the reduction algorithm used for the SDD sondes was in error. This error caused errors as large as 25% at low temperatures (−60°C) and high RH (80%). Although the condition of high RH at low temperature was not common, the potential for very significant error was present in these soundings.

There appears to be less information available on the accuracy of the Vaisala humicap. Frederickson (C. G. 1995, personal communication) has done tests showing that the humicap's plastic shield is hygroscopic and creates an artificially high RH environment around the sensor if the sonde has passed through a cloud. Thus, the CLASS soundings had a high bias near saturation and potentially missed capturing moisture layers due to sluggish response above cloud layers.

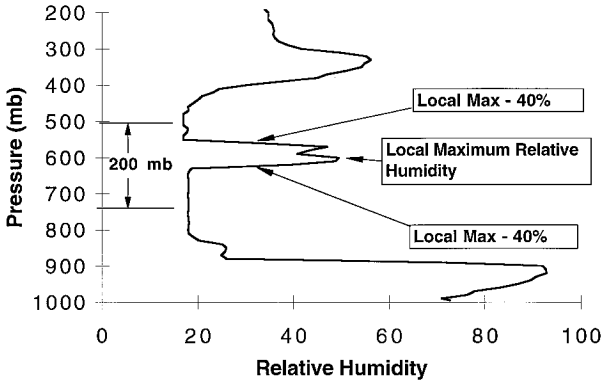

FIG. 2. An example of a moist layer, according to our definition, using the 40% humidity-change criterion.

Klein and Hilton (1987) compared the VIZ carbon hygristor and the Vaisala humicap by flying both instruments on the same sonde under different atmospheric conditions. Their report showed soundings for which the instruments were in agreement and others for which they were not. How much the degree of agreement depended on the atmospheric conditions and how much on the instruments themselves is not known. Generally, the instruments produce very similar results under clear skies and differ under cloudy conditions. Unfortunately, not enough flights were conducted to perform a statistical analysis of the relative error of the two instruments.

Although there are several potentially large sources of error, they generally occur at extreme RH values. As we will see below, the bulk of the layers found in the dataset are not at these extremes. While one reason for this behavior may be that the instruments' errors prevent finding layers at the extremes, the presence of layers away from the extremes suggests that instrument errors are not impeding markedly our search for water vapor layers. However, because of the differences in instrument response characteristics, we do present some of our results separately for the carbon hygristor (NWS) and the humicap (CLASS) soundings.

3. Definition of a moist layer

Figure 2 shows an example of a sounding containing a moist layer. Such a layer is defined as a portion of a sounding that

1) has a local maximum in RH, max(RH), at some level p_{max},
2) has RH values N% less than the local max at a level above and below p_{max} [i.e., RH = (1 − N/100) max(RH)], and
3) has all three levels within 200 mb of each other.

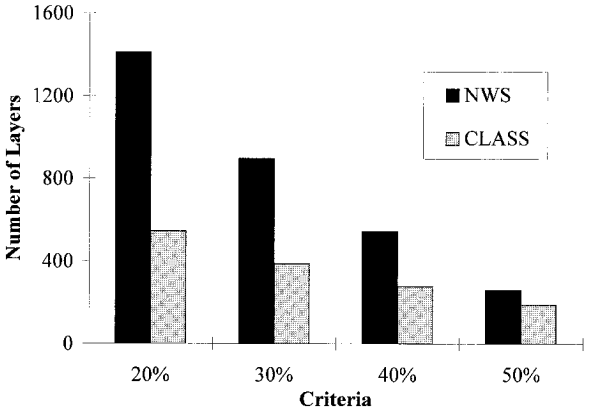

FIG. 3. The number of layers in all soundings at 0000 and 1200 UTC. Note that this is the count of all layers, not all soundings with layers.

We refer to the second criterion as the humidity-change criterion. We performed searches for layers using several different choices of N (20, 30, 40 and 50) in order to determine the dependence of layer frequencies and characteristics on N and to determine if there is a particularly appropriate choice of the humidity-change criterion. In addition, we use the levels where the relative humidity first falls to N% less than max(RH) both above and below p_{max} to determine the top and bottom edges of the layer.

4. Results

a. Abundances and distribution

Figure 3 shows the number of moist layers for each choice of the humidity-change criterion and Table 1 shows the percentage of soundings that contain at least one layer for each criterion. Note that some soundings have more than one layer and that Fig. 3 is the count of all the layers found, not of all soundings with layers. Of the soundings with layers, fewer than 6% had more than two layers.

As expected, the number of layers decreases as the humidity-change criterion becomes more stringent, but in all categories, over 440 layers are available for further analysis. Perhaps more important, even for a relatively stringent requirement that RH decrease within the layer by 40% from its maximum, roughly half the NWS soundings and three-quarters of the CLASS soundings contain at least one layer. Furthermore, the relatively linear change in the number of layers with N indicates that the values of humidity change from a layer's center to its edges are fairly evenly distributed in magnitude. If the layers typically had only small changes in RH across their depth, then there would have been an abrupt decrease to nearly zero in the number of layers as the humidity-change criterion became more stringent. Conversely, if the layers typically had large humidity changes across their depth, then the number of layers would have changed little as the criterion became more stringent.

TABLE 1. Percentage of soundings that contained at least one layer.

	Criterion			
	20%	30%	40%	50%
NWS stations	90.3	74.8	52.9	29.1
CLASS stations	90.9	86.5	76.4	60.6

We further classified layer abundances according to their max(RH) (e.g., Fig. 4). For all four choices of N that we tested, most layers found in the dataset had maximum relative humidity in the range 40%–90% and a similar overall distribution. Therefore, since the distributions are similar and since 40% far exceeds typical error estimates for RH measurement for RH between 30% and 90%, we have considered this value of the humidity-change criterion to give the representative case.

Figure 4 also shows the distribution of layers according to max(RH) for soundings taken at any time within our study region and for soundings taken only at 0000 and 1200 UTC. The two distributions are nearly the same, thus indicating that the distribution of layers was not biased by the additional soundings taken during the IOPs. As described earlier, IOPs occurred when there was an event of special interest to the STORM-FEST science team. This comparison suggests that the presence or lack of these events is not a factor in the appearance of layers. The addition of the IOP layers increases the number of soundings taken, but because the time span between soundings was so short, we do not consider them to be independent samples. Therefore, they were not used in the remainder of the analysis.

We also analyzed the 0000 and the 1200 UTC soundings separately for both instruments. We discerned no significant differences between 0000 and 1200 UTC in layer abundances or other properties that we examine

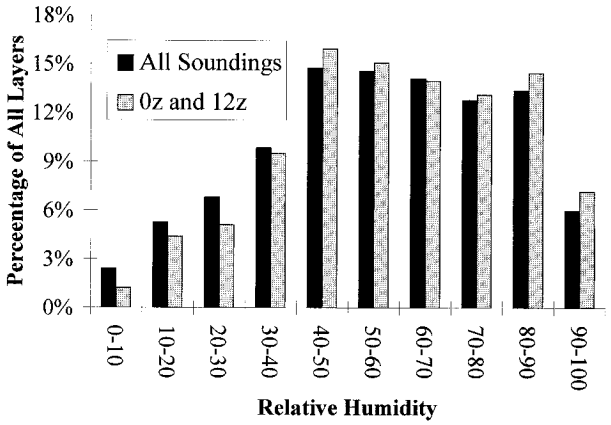

FIG. 4. The distributions of maximum RH for layers found in all soundings and those found just in the 0000 and 1200 UTC soundings, using the 40% humidity-change criterion.

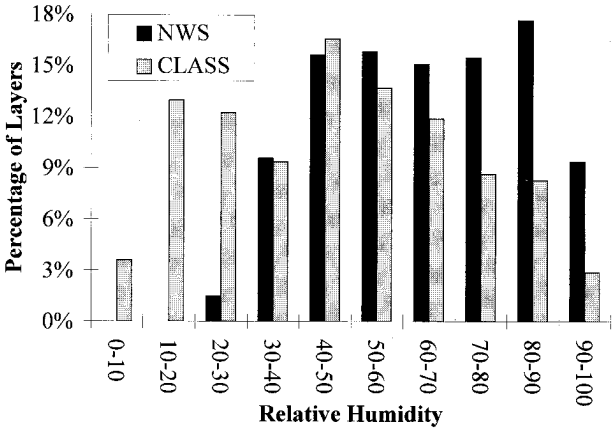

FIG. 5. The distributions of layers found in the NWS soundings and in the CLASS soundings using the 40% humidity-change criterion and only the 0000 and 1200 UTC soundings.

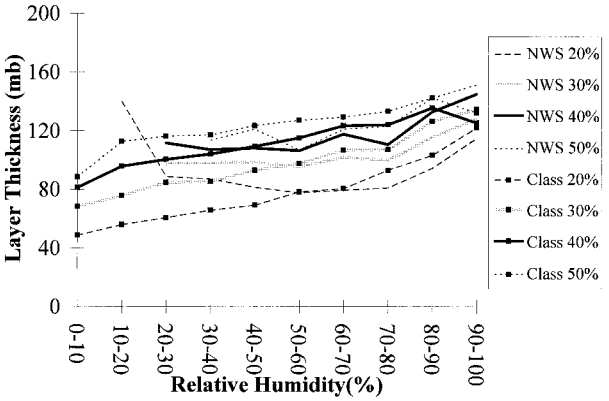

FIG. 6. Layer thicknesses as a function of maximum relative humidity for different humidity-change criteria and different instruments.

below. The behavior indicates that there is no diurnal cycle in layer properties, though one should note that these sounding times correspond to late afternoon and early morning in the central United States and so may not detect potential variability due to the diurnal solar radiation cycle. With this caveat in mind, the apparent lack of a diurnal cycle suggests that the layers observed here are controlled by large-scale dynamics and have little ongoing coupling to a diurnally varying planetary boundary layer.

The discussion of instrument errors indicates that instrument-based differences in results may appear, especially at extreme RH. This behavior appears in the distribution of layers according to their max(RH) (Fig. 5). The distribution of layers for the NWS soundings is skewed toward higher max(RH). An important contributor to the skewness is the dearth of layers with max(RH) less than 30%. Comparison with the CLASS instrument's distribution indicates that this feature is caused by the insensitivity of the VIZ carbon hygristor to humidity fluctuations below 20% RH. Both instruments show relatively few layers with max(RH) in the 90%–100% category, which may be due in part to deficiencies in both. Recall that the NWS instrument has a low RH bias near saturation (Wade and Schwartz 1993) and that the humicap can show sluggish response if it has passed through a saturated layer. Both of these factors would inhibit finding layers with maximum relative humidity near 100%. Despite the apparent instrument effects at extreme RH, there are a large number of layers found that have moderate values (40%–90%) of max(RH). The layering thus appears to be frequent even in non-cloud-bearing layers, although the two instruments give somewhat different distributions in Fig. 5.

b. Height and thickness

Figure 6 shows the average thickness of layers in the NWS soundings as a function of max(RH) and the humidity-change criterion. The lack of layers (zero thickness) at low relative humidity is again due to the low responsiveness of the VIZ carbon hygristor at RH less than 20%. The average thickness must increase as the criterion becomes more stringent, since a larger change in RH is needed to reach the layer edge. However, even at the most stringent criterion the average thickness is substantially less than the 200-mb ''window'' within which the layers had to fall, suggesting that the average layer thickness is not strongly determined by our choice of the 200-mb window. For the middle values of max(RH), the average layer thickness appears to converge with increasingly stringent humidity-change criterion to a value of about 120–140 mb. Figure 6 also shows the average layer thickness versus max(RH) when using the 40% criterion with the CLASS soundings. Except at low RH, the average layer thickness is nearly the same for the two instruments. The average layer thickness thus appears to be a fairly robust feature of the layers found using our criteria.

The average pressure level for max(RH), p_{max}, appears in Fig. 7 for each RH category, using the 40% humidity-change criterion. The figure also shows the average pressure level of the upper- and lower-layer edges. The average p_{max} is in the midtroposphere, which is consistent with the apparent lack of a diurnal cycle in layer properties. Soundings from the CLASS and NWS instruments give fairly similar average p_{max} for max(RH) above 60%, but their average p_{max} diverge as max(RH) decreases from 60%. Climatological RH in the extratropics decreases with decreasing pressure in the atmosphere (Peixoto and Oort 1992), and we might expect that the max(RH) in a layer would be governed by the same trend, that is, max(RH) would be smaller where the climatological relative humidity is smaller. Under this assumption, the behavior of the CLASS soundings would be more realistic. Recall also the findings of Marchgraber and Grote (1965), discussed earlier, who showed that the carbon hygristor element responds relatively slowly at cold temperatures to humidity changes.

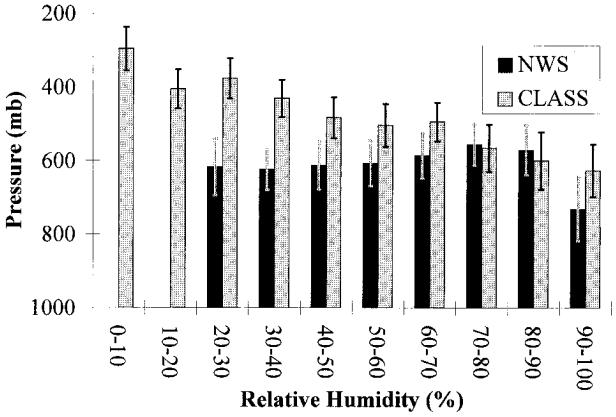

FIG. 7. Average p_{max} for the NWS layers and the CLASS layers. The ''error bars'' represent the average upper and lower edge of the layer in each RH category.

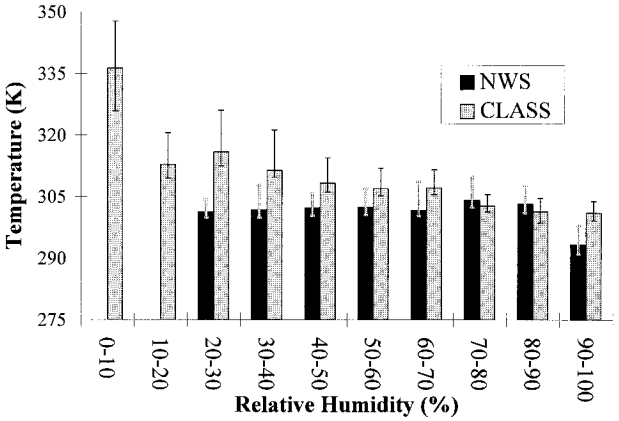

FIG. 9. Average θ_{max} for the NWS layers and the CLASS layers. The ''error bars'' represent the average upper and lower edge of the layer in each RH category.

Since temperature also generally decreases with decreasing pressure in the troposphere, at levels where the climatological relative humidity is small, the NWS instrument may not respond quickly enough to RH variations for a layer to be detected using our criteria. This possibility appears to be borne out by counting the layers detected at cold temperatures. Using the 40% humidity-change criterion, only 4% of the layers found in the NWS soundings occurred at temperatures below −40°C and only 0.6% occurred at temperatures below −50°C. In comparison, in the CLASS soundings, 15% of the layers occurred below −40°C and 2% occurred below −50°C. The tendency in Fig. 6 for layers in the NWS soundings to become thicker with lower max(RH) also suggests a sluggish instrument response at cold temperatures. While it is possible that few layers occurred in the upper troposphere over NWS instrument launch sites, the more likely explanation for the differences at low RH in Fig. 7 appears to be low instrument-sensitivity at cold temperatures in the NWS instrument.

The cold-temperature differences are also suggested by Fig. 8, which shows the p_{max} distribution for layers falling into selected max(RH) categories for both instruments. The distributions are similar in the 70%–80% range where the instruments have no apparent deficiencies. However, in the 30%–40% range, the distributions are different in a manner that is consistent with the difficulty encountered when NWS sondes measured layers at cold temperatures.

In the absence of condensation and other diabatic heating, atmospheric water vapor will maintain a constant potential temperature while being advected by atmospheric circulation. Because of this behavior, Johnson et al. (1993) have discussed extensively how the atmospheric moisture distribution may be more aligned with potential temperature levels than with pressure levels. Therefore, we have examined layer heights in isentropic coordinates. We still use the definition of a layer given in section 3, but we express the locations of p_{max} and layer edges in terms of potential temperature θ, designating the level of max(RH) as θ_{max}. Figure 9 shows the average θ_{max} and layer-edge θ levels as functions of max(RH). For comparison with Fig. 7, the temperature limits on the figure's ordinate axis are the approximate

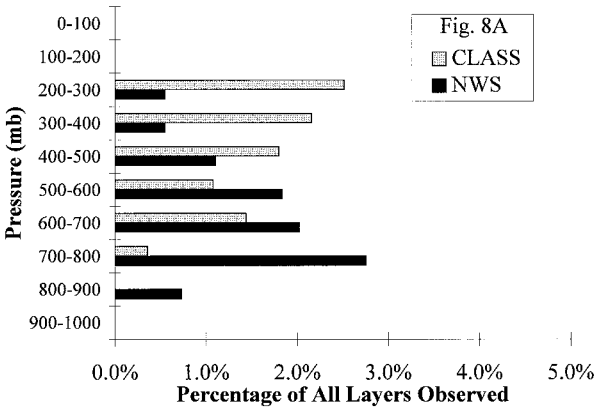

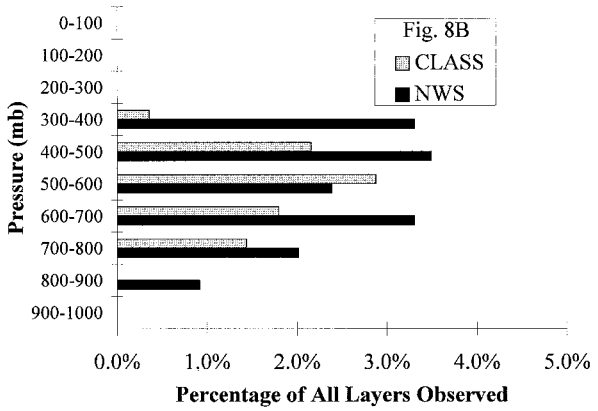

FIG. 8. Vertical distribution of p_{max} for layers with maximum RH in the range (a) 30%–40% and (b) 70%–80%. The percentages are with respect to all layers found for each instrument.

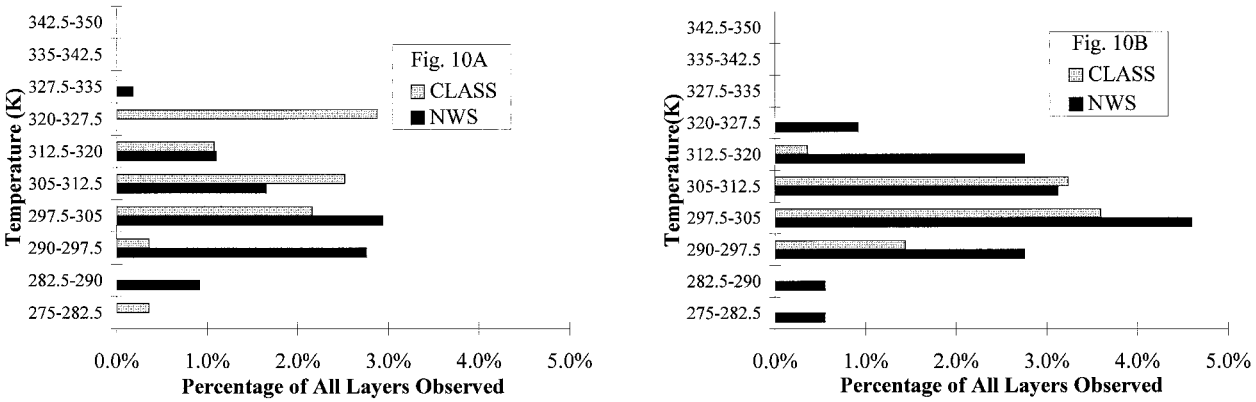

FIG. 10. Vertical distribution of θ_{max} for layers with maximum RH in the range (a) 30%–40% and (b) 70%–80%. The percentages are with respect to all layers found for each instrument.

θ(1000 mb) and θ(200 mb) for the time and central latitude of our study. Although the same qualitative differences appear in Figs. 9 and 7, the θ_{max} are confined to a relatively narrower range of values. The distribution of θ_{max} for a given max(RH) category is also more narrowly confined (Fig. 10).

The top and bottom layer edges in Fig. 7 are roughly equidistant in pressure from p_{max}, but in isentropic coordinates (Fig. 9), they are skewed with respect to θ_{max}. Thus, the pressure change from layer edge to max(RH), Δp, involves a larger change in potential temperature $\Delta\theta$ on the upper side of the layer than on the lower side—that is, the static stability ($-d\theta/dp$) is greater on the layer's upper side compared to the lower side. We examine this feature further in section 4c below.

c. Composite structure

Further insight into the structure of these layers is given by averaging similar soundings together to form composites. Figure 11 shows the results of compositing relative humidity soundings for all layers with p_{max} in the ranges 600–700 mb. The figure also shows a background relative humidity profile given by compositing all soundings at 0000 and 1200 UTC in the study domain. In the uppermost levels of the atmosphere, the background profile for the NWS soundings is much more humid than the CLASS soundings profile, consistent with the moist bias at low RH determined by Wade (1995). The background profile for NWS soundings is also slightly drier than the CLASS soundings profile near the surface, which may be due in part to the dry bias near saturation found by Wade and Schwartz (1993). However, there is also a substantial difference in the two profiles of background relative humidity in the layer 500–800 mb. This region would not seem to be strongly affected by any of the instrument biases discussed earlier, though it is possible that the moist bias in the humicap after it has passed through a cloud occurs frequently enough in these soundings that the overall average is affected significantly. Compositing of soundings with RH less than 90% RH throughout the entire sounding showed a better agreement between the NWS and CLASS soundings at lower altitudes (<800), although there were still differences in the 500–800-mb range. The CLASS stations have a distribution slightly to the north and east of the NWS stations used here, so the differences in background profiles may result from geographical variations in relative humidity. However, the precise reason for this difference is not clear.

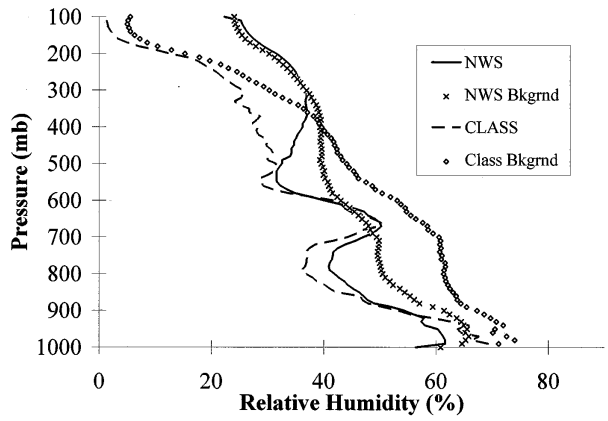

FIG. 11. Composite RH profiles using NWS and CLASS soundings containing layers that had p_{max} between 600 and 700 mb. Also shown are the composites of all NWS and CLASS soundings analyzed here.

In contrast to the background relative humidity profiles, the composites for layers with p_{max} within specified pressure intervals generally show much better agreement. Results from both CLASS and NWS soundings show that in the lower troposphere ($p > 500$ mb) the typical moist layer found here is generally a high-humidity layer in an otherwise dry atmosphere, whereas in the upper troposphere, it is simply a moist layer above a dry layer. Also, only one moist layer appears in the composites. For soundings containing a layer under the 40% humidity-change criterion, about 40% of the CLASS soundings and a fifth of the NWS soundings

TABLE 2. Layer frequency for soundings at 0000 and 1200 UTC, using the 40% humidity-change criterion.

	Number of layers			
	0	1	2	More than 2
NWS	47.1%	35.7%	14.7%	2.5%
CLASS	23.6%	34.6%	26.9%	14.9%

have more than one layer (Table 2). The lack of additional layers in the composite profiles indicates that there is no statistically consistent relationship between multiple layers in a sounding.

Composite profiles of static stability (here $-d\theta/dp$; Fig. 12) give an indication of the conditions under which the layers occur. As in Fig. 11, two types of profiles for each instrument appear in Fig. 12: averages of all 0000 and 1200 UTC soundings and averages of only those soundings that contain a layer with p_{max} inside the target pressure range. A three-point running average was used to smooth the profiles in Fig. 12. The composite static stability is relatively small around the layer's lower edge and relatively high around the layer's upper edge, consistent with the skewing of layer edges about the average height when the isentropic vertical scale is used. Since vertical velocity tends to be inversely proportional to the static stability, the composite structure indicates that relatively strong vertical motion near the layer's lower edge lifts moisture to the level of the layer, where it is then trapped by a layer of higher static stability.

d. Spatial continuity

We attempted to discern the spatial continuity of layers. Three criteria were used to indicate continuity of a layer between two stations:

1) the stations had to be within 500 km of each other,
2) the soundings examined had to be at the same time, and
3) p_{max} for a layer over one station had to lie between the upper and lower edges of a layer over the other station.

When these criteria were satisfied, the stations were considered to form a group. Other stations were added to the group if they met these criteria when paired with any of the other stations already in the group. Once all the stations in a group were found, the extreme latitudes and longitudes of the stations within the group were used to define a ''box.'' All stations falling within this box, whether they were part of the group or not, were considered for further analysis. For any box containing a spatially continuous layer according to our criteria, we counted the number of soundings linked by this layer, the number of soundings not so linked, and the number of missing soundings. We also computed the horizontal dimensions of the box. We performed our analysis using both pressure and isentropic coordinates for criterion 3 and obtained similar results using either coordinate. The results presented here used pressure as the vertical coordinate.

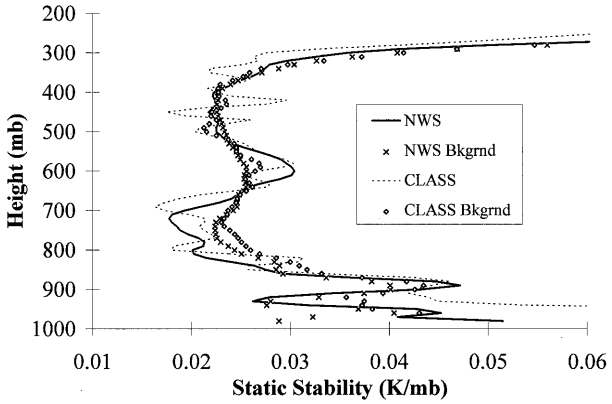

FIG. 12. Composite static stability profiles calculated from composite potential temperature profiles, using soundings with layers that have p_{max} between 600 and 700 mb. Also shown are the composites based on using all NWS and CLASS soundings analyzed here.

Table 3 shows the results of our procedure for the NWS stations, the CLASS stations, and for the combined NWS–CLASS set. Each line gives the aggregate

TABLE 3. Characteristics of spatial continuity boxes. The first column lists the group size. The second column lists the total number of soundings with a layer that was included in that line's group size. The third column lists the total number of soundings within the box that did not have a layer showing spatial continuity. The fourth column lists the number of stations within the box that did not have a successful sounding at the specified time. The last columns list the average box size.

Group size	Soundings with the layer in a group	Soundings w/o the layer	Stations w/o soundings	Box size E–W	Box size N–S
NWS soundings					
2	128	0	0	270	213
3	63	2	1	504	345
4	36	2	0	538	529
Totals	227	4	1		
CLASS soundings					
2	62	2	1	241	157
3	42	6	0	422	288
4	12	1	1	397	451
5	5	0	0	807	377
6	12	2	0	637	558
7	7	1	0	798	486
Totals	140	12	2		
NWS and CLASS combined					
2	202	11	22	244	191
3	117	15	31	401	301
4	92	35	28	505	497
5	20	9	1	563	488
6	12	5	0	670	495
7	14	5	0	979	371
8	8	2	1	926	415
Totals	465	82	83		

sounding counts and average box size for all groups with the same number of stations. The CLASS and combined soundings include groups with five, six, or seven stations, which does not occur with the NWS soundings. Only a small fraction of the soundings within any of the boxes have no layer. When comparing the number of layers that are part of a group to the total number of layers, 42% of the NWS soundings, 50% of the CLASS soundings, and, when considered together, 57% of the combined soundings are part of a group. The number of soundings that are part of a group increases for the combined dataset because of pairings between the NWS layers and the CLASS layers that are not possible when each is considered independently. However, the number of soundings within a box that had no corresponding layer also increased for the combined set. As stated earlier, the NWS soundings found layers lower in the atmosphere than did the CLASS soundings (Fig. 7). The slow response of the carbon hygristor in the NWS soundings reduced the likelihood of finding high-altitude (lower RH) layers. Additionally, the hygroscopic nature of the Vaisala humicap in the CLASS soundings reduced the number of high RH layers found (Fig. 5), due to trapping of moisture after passing through a cloud. Therefore, it is to be expected that each instrument, when considered individually, is able to find a certain degree of spatial continuity, but when considered together their individual weaknesses increase the likelihood that nearby soundings by one instrument may not contain a layer that was found by the other instrument.

As noted in the introduction, atmospheric moisture can form elongated structures. If this is occurring often during STORM-FEST, then the success of finding spatial continuity within a layer is dependent upon the spatial orientation of the stations matching the orientation of the elongated moisture concentration. On the basis of the STORM-FEST dataset, we cannot assess the elongation of the water vapor layers and, hence, how much such a structure might impede our attempt to determine spatial continuity. However, there appears to be some degree of resolvable spatial continuity in the layers, according to our criteria. Only about half of the soundings fall into a group, though, suggesting that the station network used here, with average station spacing of 340 km, may just barely resolve the typical horizontal scale of the water vapor layers.

5. Conclusions

The STORM-FEST composite dataset was analyzed for evidence of relatively thin layers of atmospheric moisture. Since two different types of rawinsondes were used during STORM-FEST, the measuring characteristics of the two instruments were reviewed. Although both instruments have some weaknesses, a substantial number of moist layers are found in soundings produced by both. The deficiencies of the humidity instruments are more likely to result in actual layers being missed rather than spurious layers being generated, a behavior apparent in our results. The number of layers found depended on how much we required relative humidity to decrease from the interior to the edge of the candidate layer, but even with a stringent, 40% difference, 58% of the soundings had at least one layer.

The layers were categorized according to their maximum relative humidity. The distributions indicate that the majority of layers occur at max(RH) values of 40%–70%, although both instruments had some difficulties accurately measuring high humidities (>95%), which could bias the statistics against finding a substantial number of high-humidity layers. The average height of the layers shows that the majority of the layers were in the midtroposphere and that an isentropic vertical scale may be better suited for discerning them than an isobaric scale. Composite vertical profiles of RH and static stability using soundings with layers occurring at the same level indicated that a sounding typically has only a single layer and that the layers are formed by a trapping of moisture below a level of relatively strong static stability. Roughly half of the layers showed spatial continuity with neighboring layers. On this basis, it appears that the horizontal resolution of the network was barely fine enough to resolve any spatial continuity. A typical horizontal spatial scale for these layers would then be a few hundred kilometers.

The STORM-FEST dataset covers only a 6-week period in the central United States. However, the weather during this period was fairly typical for winter in the United States, so that the behavior of water vapor observed here may be representative of extratropical climatology. If this is the case, then the implications of these results for numerical weather prediction is significant. Atmospheric moisture observed in STORM-FEST can have sharp gradients in the vertical. Other studies cited earlier indicated that sharp gradients in the horizontal are also common, which would be consistent with the scales of spatial continuity emerging here. Accurate representation of atmospheric moisture in models is therefore difficult to attain for two reasons. First, accurate measurement for initial and boundary conditions appears to need finer resolution, especially in the horizontal, than is often archived. Instrumentation weaknesses exhibited here, however, could undermine attempts to archive atmospheric moisture at higher vertical resolution. Second, the sharp gradients and small scales in both the vertical and the horizontal pose stringent requirements for numerical resolution. The regions in which these layers appear are not confined to one predictable region that can be defined a priori to receive higher resolution, such as through grid refinement. We have shown that the distribution of layers in the STORM-FEST dataset occurs not only over wide RH ranges, but also throughout the troposphere from at least as low as 900 mb and to at least as high as 200 mb. Adequate resolution of these layers on a numerical model would require substantially higher vertical resolution

in the region 300–800 mb than is often used by global or mesoscale models. More sophisticated means of resolving these small-scale, widely varying structures in numerical models may be necessary. A need for further study of the layering over broader space and timescales is also indicated by this study.

Acknowledgments. This research was supported in part by U.S. Department of Energy Grant DE-FG02-92ER6147 and U.S. National Science Foundation Grant ATM-9123552. Additional support was provided by the Iowa Agriculture and Home Economics Experiment Station, Ames, Iowa, Project No. 3153, supported by Hatch Act and State of Iowa funds. Data were obtained from the STORM-FEST World Wide Web site, http://www.ofps.ucar.edu/data/fest/docs/sounding_comp. We thank Steve Williams at UCAR's Office of Field Project Support and Charles Wade of NCAR for answering our questions about rawinsonde humidity measurements.

REFERENCES

Coakley, J. A., Jr., and F. P. Bretherton, 1982: Cloud cover from high resolution scanner data: Detecting and allowing for partially filled fields of view. *J. Geophys. Res.,* **87,** 4917–4932.

——, and D. G. Baldwin, 1984: Towards the objective analysis of clouds from satellite imagery data. *J. Climate Appl. Meteor.,* **23,** 1065–1099.

Cunning, J. B., and S. F. Williams, 1993: *STORM Fronts Experiment Systems Test (STORM-FEST) Operations Summary and Data Inventory.* NOAA, 389 pp.

Danielsen, E. F., 1968: Stratospheric-tropospheric exchange based on radioactivity, ozone and potential vorticity. *J. Atmos. Sci.,* **25,** 502–518.

Elliott, W. P., and D. J. Gaffen, 1991: On the utility of radiosonde humidity archives for climate studies. *Bull. Amer. Meteor. Soc.,* **72,** 1507–1520.

Gyakum, J. R., 1987: Evolution of a surprise snowfall in the United States Midwest. *Mon. Wea. Rev.,* **115,** 2322–2345.

Johnson, D. R., T. H. Zapotocny, F. M. Reames, B. J. Wolf, and R. B. Pierce, 1993: A comparison of simulated precipitation by a hybrid isentropic–sigma and sigma models. *Mon. Wea Rev.,* **121,** 2088–2114.

Klein, G., and A. Hilton, 1987: An intercomparison of the Vaisala humicap and the VIZ carbon hygristor under operational conditions. Data Acquisition Services Branch, Atmospheric Environment Service, Environment Canada, Tech. Rep. TR16, 32 pp. [Available from C. Wade, National Center for Atmospheric Research, P.O. Box 3000, Boulder, CO 80307.]

Kuettner, J., 1959: The band structure of the atmosphere. *Tellus,* **11,** 267–294.

Marchgraber, R. M., and H. H. Grote, 1965: The dynamical behavior of the carbon humidity element ML-476. *Humidity and Moisture I,* R. E. Ruskin, Ed., Reinhold Publishing, 331–345.

Molnar, G., and J. A. Coakley Jr., 1985: Retrieval of cloud cover from satellite imagery data: A statistical approach. *J. Geophys. Res.,* **90,** 12 960–12 970.

Newell, R. E., N. E. Newell, Y. Zhu, and C. Scott, 1992: Tropospheric rivers?—A pilot study. *Geophys. Res. Lett.,* **12,** 2401–2404.

——, and Coauthors, 1996: Vertical fine-scale atmospheric structure measured from NASA DC-8 during PEM-West A. *J. Geophys. Res.,* **101,** 1943–1960.

Peixoto, J. P., and A. H. Oort, 1992: *Physics of Climate.* American Institute of Physics, 520 pp.

Pratt, R. W., 1985: Review of radiosonde humidity and temperature errors. *J. Atmos. Oceanic Technol.,* **2,** 404–407.

STORM, cited 1996: STORM Sounding Composite Dataset. [Available on-line at http://www.ofps.ucar.edu/data/fest/docs/sounding_comp]

Wade, C. G., 1994: An evaluation of problems affecting the measurement of low relative humidity on the United States radiosonde. *J. Atmos. Oceanic Technol.,* **11,** 687–700.

——, 1995: Calibration and data reduction problems affecting national weather service radiosonde humidity measurements. Preprints, *Ninth Symp. on Meteorological and Instrumentation,* Charlotte, NC, Amer. Meteor. Soc., 37–42.

——, and B. Schwartz, 1993: Radiosonde humidity observations near saturation. Preprints, *Eight Symp. on Meteorological Observations and Instrumentation,* Anaheim, CA, Amer. Meteor. Soc., 44–49.

Waugh, D. W., and R. A. Plumb, 1994: Contour advection with surgery: A technique for investigating finescale structure in tracer transport. *J. Atmos. Sci.,* **51,** 530–540.

Welander, P., 1955: Studies on the general development of motion in a two dimensional, ideal fluid. *Tellus,* **7,** 141–156.